

Numerical Investigation on Toggled Actuator Forces in Active Vibration Control System

Seyyed Farhad Mirfakhraei¹, Gholamreza Andalib^{2*}, Ricky Chan³

¹ Ph.D. of Structural Engineering, Department of Civil and Infrastructure Engineering, Faculty of Civil Engineering, University of RMIT, Melbourne, Australia.

² Ph.D. of Water and Hydraulic Structure, Department of Water Resource Engineering, Faculty of Civil Engineering, University of Tabriz, Tabriz, Iran.

³ Associate Professor, Department of Civil and Infrastructure Engineering, Faculty of Civil Engineering, University of RMIT, Melbourne, Australia.

*Corresponding author's Email: gholamreza.andalib@gmail.com

(Date of received: 08/10/2018, Date of accepted: 22/03/2019)

ABSTRACT:

In this paper a numerical investigation of installation of actuator in a toggle configuration for decreasing of active control forces in engineering structures has been carried out. During the past two decades, researchers have been focused to prevent the vibration of tall building from strong earthquakes. For achieving this purpose, they applied either massive conventional bracing or passive energy dissipation dampers. Subsequently, they developed active control systems in structures to resist against the high seismic loads. However, this later method eventuates installing massive actuators in building which are not only very costly and uneconomically but also needs large electricity power. In this research, using by known earthquakes, investigation of the effects of the toggle configuration on actuator forces has been performed numerically. For numerical investigation, active tendon control system was selected as a comparison. The numerical investigation shows significant reduction in actuator forces through using toggle configuration. Finally, comparing results through the numerical processe express high matching that relies on mitigation of control forces in the toggled active model.

Keywords: Active control system, Control forces, Structural active vibration control

1- Introduction

Utilization of active control systems for resisting against seismic loads such as strong earthquakes or intensive wind gust turbulences loads on structures has been developed in the past two decades[1-5]. Producing of high strength material and achieving the reliable and accurate structure analysing software caused to be built more tall and flexible buildings[2]. The more strength against the excitation, the more structure strength and ductility is required. Obviously, providing high strength and ductile construction materials are very costly. Using the bigger cross sections for achieving to the higher structure strength, however, attracts more seismic force onto these members. Consequently, they will require even bigger sections. This process is endless spiral design. One of the important advantages of smart structures is to overcome to this problem. The previous researches and practical installations proved their efficiency to protect the structures against the seismic excitations. In the structures once multiple modes are determinant in structure respond, need for more powerful and adaptive system to prevent structure from very large excitations and damages will be more essential [6]. There are many real implementation of active control systems in the world [7-16]. Also, utilizing of this system in the large

civil engineering structures is being expanded [6]. By increasing the number of tall buildings in whole of the world, to achieve high reliability and safety, using of active control systems will be inevitable [2].

Undoubtedly, finding of optimum control force that can achieve allowable structural response is one of the most important tasks in active control systems. The actuators' power and unit cost as well as their maintenance expenses are very important factors from economically and efficiency point of view [17-19]. The mitigation of control forces in active control systems have been emphasized by the recent researchers as an efficiency factor in reduction of structural response[2, 20, 21]. Also, it should be mentioned that the importance of actuator positions in active control system to reduce the structural response has been quoted [1,17,18,20 and 22].

The toggle configuration has been recognised as an efficient layout for viscous damper installation in a structural system having a large stiffness. Employing the concept of energy dissipation has been explored via devices installed in the conventional earthquake-resistant structures and can protect the structures effectively against seismic excitations [23, 24]. Fluid viscous dampers are devices which can strongly enhance the damping ratio and, consequently, mitigate the structural vibrations caused by excitation [25-27]. Also, in recent years, the practical installation of these types of dampers in civil engineering structures can be found in the work of [28]. However, there is a particular challenge in installing various dampers in a stiff structural system. The reason is that the seismic structural responses i.e. storey displacement and velocity, are small compared with a typical flexible structure. Therefore, viscous dampers with a substantial force capacity and a massive damping coefficient are needed for dissipating a relevant amount of energy and attaining an intended damping ratio. Then, the implementation of viscous damping devices in structures having more stiffness will be less efficient than installation in a structure having an acceptable flexibility.

Considering the latter challenge, researchers have recently suggested some configurations for installing the dampers to enhance the displacements and velocities in dampers. Taylor in U.S. Patent Nos.5870863 and 5934028, 1996 (Taylor, 1999) has suggested the "toggle-brace-damper" system. An investigation into the "toggle-brace-damper" system has been performed by [29]. In this investigation, the ability of this system to magnify the damper's axial displacements and the efficiency of energy dissipation has been verified through a cyclic loading and shaking table tests in a SDOF steel model. Aiming to have more free architectural spaces in buildings, a similar system to toggle-brace-damper, called the "scissor-jack-damper" system, has been introduced [30]. This system can also magnify the damper displacements and velocity and enhance the efficiency of energy dissipation in the frames having less occupied architectural spaces. Some practical examples of using the toggle-brace-damper systems in constructions have been outlined [29]. One such practical example, that is, 111 Huntington Avenue in Boston, Mass., has a lower toggle system directly connected to the beam-column joints, which is different from the configuration proposed by Constantinou [29]. Moreover, Hwang [31] have investigated the effect of the lower and upper toggle system in the latter system and the facilitation of the practical implementation of the dampers.

In this research, the upper toggle system that is directly connected to the beam-column joints has been suggested for installation in an active control system. Unlike the aforementioned toggle configurations which have been utilized in the passive systems, this research performs investigations to find the effect of the toggle configuration in the mitigation of the active control forces. Considering the importance of small control forces to attain small-sized actuators for preventing significant earthquake excitations in a structural active control system, an actuator is installed in the toggle configuration in an active control system in the single degree of freedom (SDOF) bending frame. A numerical investigation are performed using the mentioned system to investigate effect of this configuration on the actuator forces respect to the different earthquake excitations.

2- SDOF Toggle Configuration

A single-degree-of-freedom shear frame with one span and one storey is considered, as shown in Fig.1, where the actuator has been installed in a toggle configuration, i.e. OB member. OA and OC are the members considered to be axially rigid. The members of OA and OC are connected to the main frame at points A and C and to each other at point O. These connection points are hinged connections. It means that these two members can rotate freely about a normal axis passed through point A, C and O in the plane of members OA and OC. Also, the figure shows a response sensor has been implemented at the top of the frame. Furthermore, there is a controller installed in this system that can determine the control signals by its own algorithm based on the received structural response data measured by the sensor.

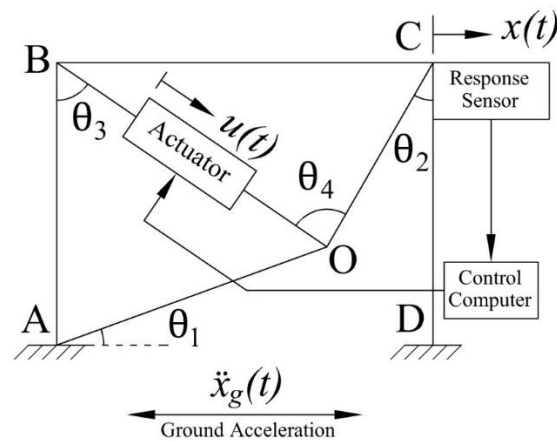


Fig.1. Toggle configuration in active control system.

Figure 2 shows the relevant forces in the toggle configuration in the active control system. As can be seen from the figure, the structural response i.e. velocities and displacements due to earthquake forces is measured by the sensor. Then, the measured information is sent to the controller. Furthermore, the controller determines the control forces based on its algorithm and sends the signals to the actuator. Finally, the actuator applies the control force, through members OA and OC, to the main structure in order to neutralize the effect of that disturbance in the opposite direction.

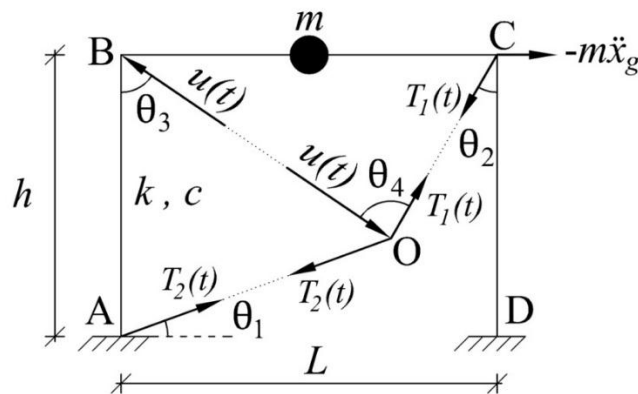


Figure 2. Forces in active toggle control system.

In this figure $u(t)$ is actuator force, $T_1(t)$ and $T_2(t)$ are tension or compression forces in members OA and OC with regard to the direction of the displacement, m is a lumped mass of the structure and \ddot{x}_g is the earthquake acceleration.

3- Motion equation in active Toggle control system

The motion equation of the toggle system can be obtained through the following process. Considering Figure 2, the equilibrium of horizontal and vertical forces in the hinge O in a time instant can be written as follows, respectively:

$$T_1(t) \sin \theta_2 - T_2(t) \cos \theta_1 + u(t) \sin \theta_3 = 0 \quad (1)$$

$$T_1(t) \cos \theta_2 - T_2(t) \sin \theta_1 - u(t) \cos \theta_3 = 0 \quad (2)$$

Where, $u(t)$ is actuator force, $T_1(t)$ and $T_2(t)$ are tension forces in the members of OA and OC, respectively. Also, the angles of θ_1 , θ_2 and θ_3 have been shown in Figure 2. $T_1(t)$ and $T_2(t)$ can be derived by solving Equations 1 and 2 simultaneously indicated as below:

$$T_1(t) = \alpha_1 u(t) \quad (3)$$

$$T_2(t) = \alpha_2 u(t) \quad (4)$$

Where, α_1 and α_2 are as follows:

$$\alpha_1 = \cos(\theta_1 - \theta_3) / \cos(\theta_1 + \theta_2) \quad (5)$$

$$\alpha_2 = \sin(\theta_2 + \theta_3) / \cos(\theta_1 + \theta_2) \quad (6)$$

If m , c , and k are the lumped mass, damping and stiffness of the structure, respectively, the motion equation of the system considering the concept of dynamic equilibrium can be written as follows:

$$m\ddot{x}(t) + c\dot{x}(t) + kx(t) + u(t) \sin \theta_3 + T_1 \sin \theta_2 = -m\ddot{x}_g(t) \quad (7)$$

After substituting Equation 3 into Equation 7 and using Equation 5, the motion equation for the toggle system is derived as:

$$m\ddot{x}(t) + c\dot{x}(t) + kx(t) = -\alpha u(t) - m\ddot{x}_g(t) \quad (8)$$

While,

$$\alpha = \sin\theta_3 + \frac{\cos(\theta_1 - \theta_3)}{\cos(\theta_1 + \theta_2)} \sin\theta_2 \quad (9)$$

Equation 8 **Error! Reference source not found.** is the motion equation for an active control system in the toggle configuration, illustrated in Figure 2. In this formula, m is the mass in kNs^2/m , c is the damping coefficient in $kN s/m$, k is the stiffness in kN/m , $u(t)$ is the actuator force in kN , $\ddot{x}_g(t)$ is the earthquake acceleration in m/s^2 and α is the toggle coefficient, which depends on the angles of θ_1 , θ_2 and θ_3 . Equation 8 dictates the motion of the system for toggle configuration. From the point of view of control system design, the objective is to minimize the displacement $x(t)$ by changing the force $u(t)$. The variable $\ddot{x}(t)$ is the acceleration generated by an earthquake excitation, which is considered to be disturbance.

4-Efficiency of active Toggle control system

As mentioned already, one of the specific objectives of this research is the reduction of the required active control forces applied by the actuators. This reduction of control forces is selected as an efficiency factor in the active toggle control system. Therefore, for investigating the efficiency of the active control system having a toggle configuration, two single-degree-of-freedom systems with identical mass, damping and stiffness values have been chosen. The first system has the active control system in a toggle configuration and the second one has a tendon control system [6], as indicated in Figures **Error! Reference source not found.**3 and 4, respectively. The motion equation of the active toggle control system, which has been already achieved, is restated here, as follows:

$$m\ddot{x}(t) + c\dot{x}(t) + kx(t) = -\alpha u_{Toggle}(t) - m\ddot{x}_g(t) \quad (10)$$

The motion equation of the active tendon control system, indicated in Figure 4, can be derived as below, while the frame has a single-degree-of-freedom [6]. Notice that in this comparison, the mass, damping and stiffness of both frames are assumed to be identical.

$$m\ddot{x}(t) + c\dot{x}(t) + kx(t) = -u_{Tendon}(t) - m\ddot{x}_g(t) \quad (11)$$

Using Equations **Error! Reference source not found.**10 and 11, the relationship between the actuator forces related to the toggle and tendon systems in a time instant is obtained as follows:

$$u_{Toggle}(t) = \left(\frac{1}{\alpha}\right) u_{Tendon}(t) \quad (12)$$

Where α is the toggle coefficient, defined in Equation 9.

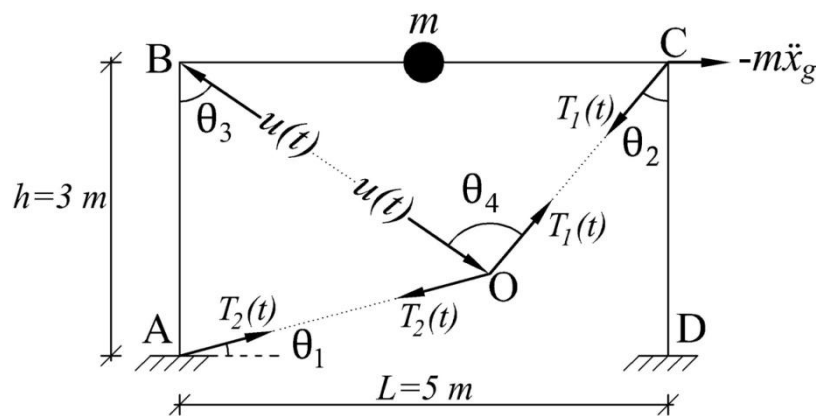


Figure 3. Active toggle control system.

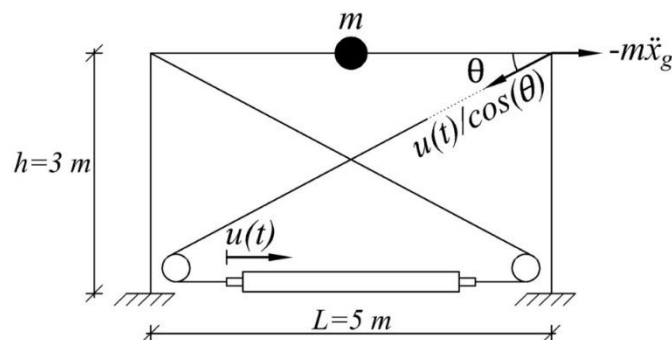


Fig.4. Active tendon control system.

Equation 12 **Error! Reference source not found.** shows that the active toggle control system is more efficient than the active tendon control system if α is greater than unity. Therefore, for proving that, the variation of α for all the acceptable values of θ_1 should be investigated. For this purpose, the effect of toggle coefficient α in the active toggle control system has to be studied. In the next section, it will be proved that all values of α are greater than unity. Therefore, the control forces in the toggle control system are α times smaller than the control forces in the tendon control system for stabilizing the frame against the same excitation. Fig.5 shows that, when θ_1 approaches to its maximum values, the toggle coefficient α increases rapidly. However, the toggle establishment criterion, i.e. $\theta_1 + \theta_2 < 90^\circ$, as well as practical restrictions, should be considered during the design process.

5- Effect of Toggle coefficient α

In the toggle configuration indicated in Figure 2, for any given value for θ_1 , the corresponding value for θ_2 is calculated using the geometry of the system. In other words, the proper establishing of the motion equation in the toggle system depends on suitable values for θ_1 to θ_3 and L_1 . Otherwise, the toggle configuration of the active control system will no longer be valid. It should be mentioned that the system works as a toggle configuration in the active control system if $\theta_1 + \theta_2 < 90^\circ$. In the toggle configuration, θ_1 and L_1 are independent values. It means that all other geometrical characteristics can be calculated from the geometry of the system after selecting values for θ_1 and L_1 . Considering Fig.5, these values can be calculated by the following formulas:

$$L_3 = \sqrt{(h^2 + L_1^2 - 2hL_1 \cos(90 - \theta_1))} \quad (13)$$

$$\theta_3 = \arccos\left(\frac{-L_1^2 + h^2 + L_3^2}{2hL_3}\right) \quad (14)$$

$$\theta_5 = 90 - \theta_3 \quad (15)$$

$$L_2 = \sqrt{(L^2 + L_3^2 - 2LL_3 \cos(\theta_5))} \quad (16)$$

$$\theta_6 = \arccos\left(\frac{-L_3^2 + L^2 + L_2^2}{2LL_2}\right) \quad (17)$$

$$\theta_2 = 90 - \theta_6 \quad (18)$$

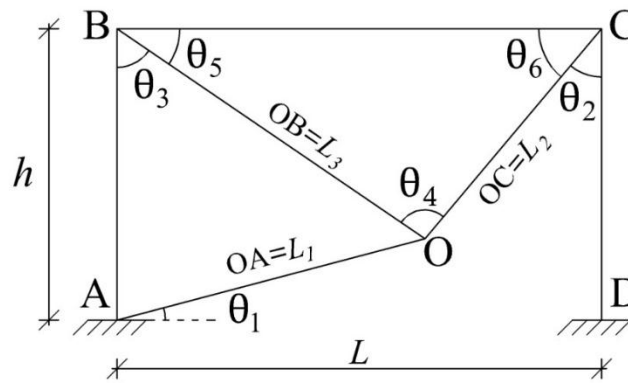


Fig.5. Toggle configuration parameters in SDOF active control system.

The effect of variations of θ_1 and L_1 is shown, in Equation 8, in the coefficient of α , which has been multiplied as a direct factor to the actuator force. Hence, numerically finding variations of α with respect to θ_1 through Equation 9, would be more straightforward. Therefore, considering $h=3.0$ m and $L=5.0$ m in Figure 3, the variations of α with respect to θ_1 having different L_1 can be determined. Notice that in this calculation, the maximum values of θ_1 and θ_2 can be easily obtained using Figure 3. However, as a toggle establishment criterion mentioned earlier, the inequality of $\theta_1 + \theta_2 < 90^\circ$ must be satisfied. Then, the maximum values for θ_1 and θ_2 are derived 30.96° and 59.04° , respectively. Using Equation 9, all values of α have been plotted with respect to all acceptable values of θ_1 while L_1 varies from 1.0m to 4.0m. These results are indicated in Fig.6.

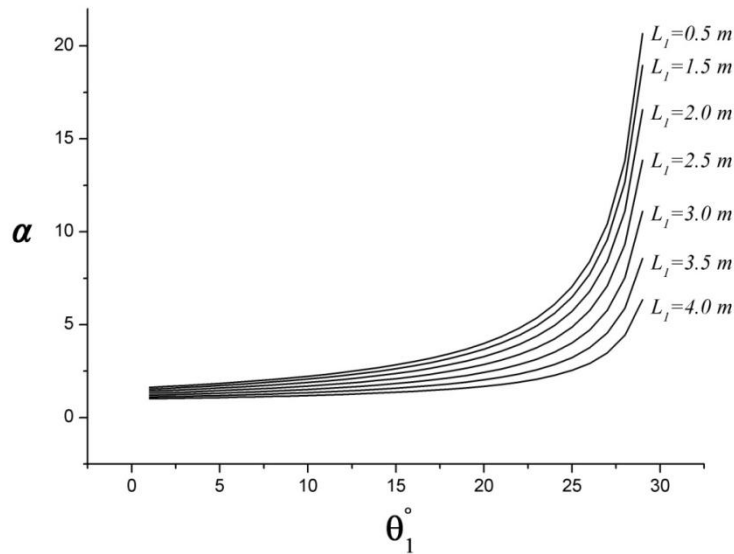


Fig.6. Variations of α with respect to θ_1 with different L_1 .

Fig.6 shows that all values of α are greater than unity. Therefore, referring to previous section regarding the efficiency of the toggle system compared to the tendon system, these values of α , which are greater than unity, prove that the Toggle system is more efficient than the tendon system.

6- Effects of θ_1 and L_1 in Toggle configuration

It was noted in Section 5 that θ_1 and L_1 are independent values in the toggle configuration. This means that these two parameters should be preselected prior to the design of the active control system in a toggle configuration. This is why selecting the suitable values for these two parameters is very important. Fig.6 is the same figure which shows the effects of both θ_1 and L_1 in the toggle system. This figure indicates that, when the value of θ_1 approaches its maximum value, the toggle coefficient of α increases rapidly. In other words, the toggle system acts more efficiently in θ_1 s that are close to their maximum values. Although reaching the higher toggle coefficient is desirable, the toggle establishment criterion $\theta_1 + \theta_2 < 90^\circ$ and construction restrictions have to be taken into consideration as well in choosing θ_1 . Also, the results indicated in Fig.6 can help designers to choose the optimum value for L_1 based on their construction specifications and restrictions. It is clear from Fig.6 that the smaller L_1 generates the greater α . Therefore, to have the more efficient toggle system, the smaller L_1 should be selected.

7- Effects of frame span length in Toggle configuration

To investigate the effects of variations of the frame span length, L , on the toggle coefficient, the numerical method similar to that utilized in Section 5 is applied here. For this, considering $h=3.0$ m and $L_1=1.5$ m in Figure 3, the variations of α with respect to θ_1 having different L can be determined. The result has been printed in Fig.7.

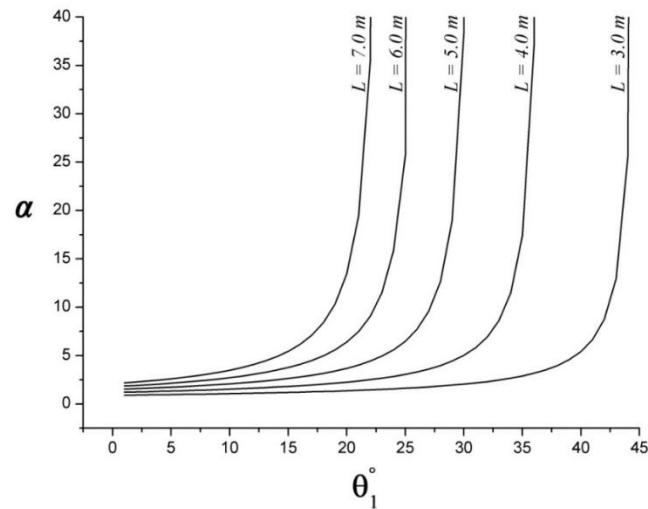


Fig.7. Variations of α with respect to θ_1 with different L .

Fig.7 shows that the greater span produces the bigger toggle coefficient of α while θ_1 varies from zero degrees to its relevant maximum value. This figure proves that, during the design procedure in the active toggle control system, it is desirable to select the frames with bigger spans.

8- Effects of frame height in Toggle configuration

To investigate the effects of variations of the frame height, h , on the toggle coefficient, the same numerical method used in Section 5 is performed here. Thus, assuming $L=6.0\text{ m}$ and $L_1=1.5\text{ m}$ in Figure 3, the variations of α with respect to θ_1 having different h can be calculated. These results have been indicated in Fig.8.

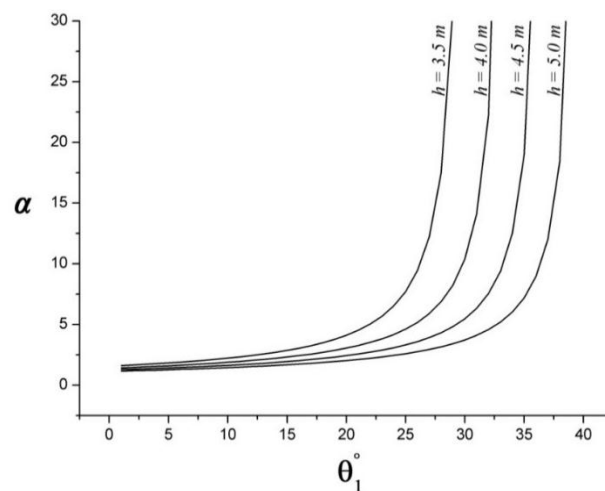


Fig.8. Variations of α with respect to θ_1 with different h .

Fig.8 expresses that the greater height produces the smaller toggle coefficient of α while θ_1 varies from zero degrees to its relevant maximum value. This figure proves that, during the design procedure in the active toggle control system, it is beneficial to select the lowest frame height possible.

9- Numerical analysis

9.1. Methodology

Referring to the specific objectives mentioned in this research, the reduction of the required control forces in the active toggle control system is investigated in this section through a numerical analysis. The outline of this procedure is as follows:

- 1-Defining a single-degree-of-freedom active toggle control system, indicated in Fig.9 as a main unit.
- 2-Selecting a single-degree-of-freedom active tendon control system, shown in Fig.10 as a comparison unit.
- 3-Determining the optimum value for toggle coefficient α based on the property of the toggle configuration.
- 4-Introducing the installed feedback control layout in the both systems.
- 5-Presenting the implemented algorithm in both systems.
- 6-Choosing the earthquake acceleration data.
- 7-Obtaining the state form of the motion equation for both systems.
- 8-Deriving the gain matrix utilizing the *LQR* function in MATLAB.
- 9-Calculating the state vector using *LSIM* function in MATLAB.
- 10-Calculating the control forces for both systems.
- 11-Comparing the results using the generated graphs.

9.1.1. Active Toggle control system

In this approach, a single-degree-of-freedom frame with an active toggle control system is selected, as indicated in Fig.9. The structure, actuator, sensor and controller in this process are assumed to be linear [6, 32-35].

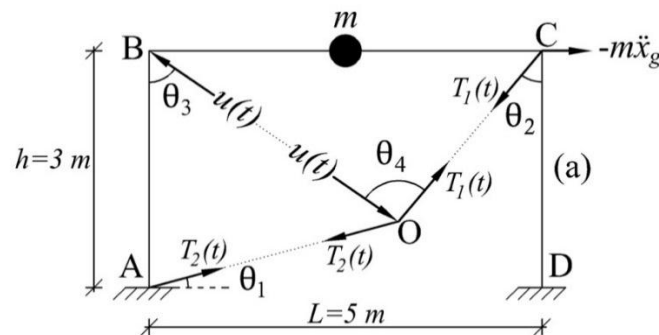


Fig.9. Active toggle control system.

9.1.2. Specifications of Toggle system

In this numerical analysis, the columns are 150UC23.4 and the beam is 180UB22.2. The relevant specifications are listed in the below table.

Table 1. Specifications of toggle system.

Specification	Value	Unit
L	5	m
h	3	m
m	12	ton
c	3.4	kNs/m
k	589	kN/m
I_b	15.3×10^6	mm^4
I_c	3.98×10^6	mm^4
ρ	1.153	—
E	200	GPa
ω_n	7	rad/sec
T_n	0.898	sec

Assuming the damping ratio is equal to 2% for a steel frame, i.e. $\zeta = 2\%$, the stiffness, damping, natural frequency and period of the assumed frame has been calculated using the following formulas, respectively [36]:

$$k = \frac{24EI_c}{h^3} \frac{12\rho+1}{12\rho+4} \quad (19)$$

$$\rho = \frac{EI_b/L}{2EI_c/h} \quad (20)$$

$$c = 2\zeta\sqrt{km} \quad (21)$$

$$\omega_n = \sqrt{\frac{k}{m}} \quad (22)$$

$$T_n = \frac{2\pi}{\omega_n} \quad (23)$$

In the above mentioned equations, L , h , m , k , c , I_b , I_c , ρ , E , ζ , ω_n and T_n are the frame span, height, mass, stiffness, damping, the moment of inertia of the beam, the moment of inertia of the columns, the beam-to-column stiffness ratio, modulus of elasticity of steel, the damping ratio of the frame, natural frequency and natural period, respectively.

9.1.3. Active tendon control system

As a comparison unit, an active tendon control system with the same specifications as those indicated in Table 1 is considered. This system has been shown in Fig.10 [6]. All the characteristics of this system are assumed to be similar to the toggle system, apart from the active toggle control.

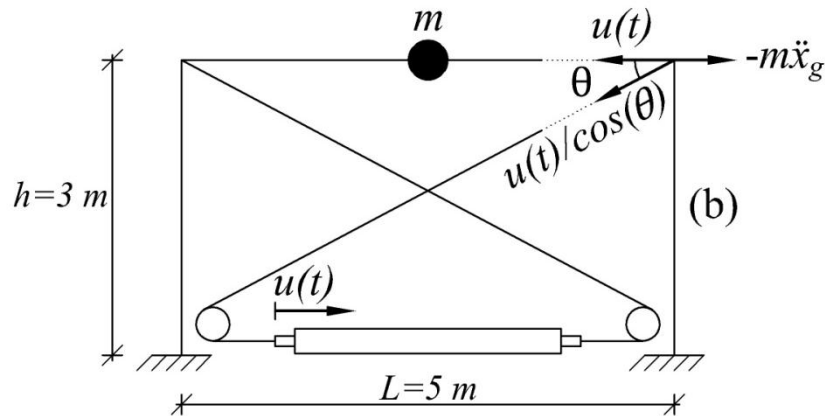


Fig.10. Active tendon control system.

9.1.4. Specifications of tendon system

The specifications of this system have been assumed to be identical to the active toggle control system. These characteristics have been shown in **Error! Reference source not found.**

9.1.5. Determination of optimum Toggle coefficient α

It was proven in the previous sections that the values of actuator forces decrease by increasing toggle coefficient α . On the other hand, Fig.6 shows that the toggle coefficient of α increases by diminishing the length of the lower brace L_1 . Therefore, the smaller values of L_1 produce the bigger values of α , which results in smaller control forces. For selecting the optimum values of α , both the establishment criterion for the toggle configuration and the construction limitations should be taken into account. Accordingly, referring to Fig.6, θ_1 and L_1 are selected as 27° and 1.5 m , respectively. As mentioned in Section 5, θ_1 and L_1 are independent values. Therefore, the other characteristics of the system can be obtainable after choosing the optimum values for θ_1 and L_1 . All the other specifications needed for calculating the optimum toggle coefficient in this numerical analysis have been calculated utilizing the equations expressed in Section 5 and indicated in Table 2. Finally, the toggle coefficient of α can be derived using by Equation 9 **Error! Reference source not found.**

Table 2. Required characteristics for calculating optimum α .

Specification	Value	Unit
L_1	1.5	m
L_2	4.33	m
L_3	2.68	m
θ_1	27	degree
θ_2	57.7	degree
θ_3	30	degree
θ_4	87.7	degree
θ_5	60	degree
θ_6	32.3	degree
α	9.6	—

9.1.6. Feedback law in closed-loop control

State form of motion equation of the control system can be written as follows [6]:

$$[\dot{Z}(t)] = [A][Z(t)] + [B_u][u(t)] + [B_r][\ddot{x}_g(t)] \quad (24)$$

Where,

$$[\dot{Z}(t)] = \begin{bmatrix} \dot{x}(t) \\ \dot{\ddot{x}}(t) \end{bmatrix}_{2 \times 1} \quad (25)$$

$$[A] = \begin{bmatrix} [0] & [I] \\ -[M]^{-1}[K] & -[M]^{-1}[C] \end{bmatrix}_{2 \times 2} \quad (26)$$

$$[B_u] = \begin{bmatrix} [0] \\ [M]^{-1} \end{bmatrix}_{2 \times 1} \quad (27)$$

$$[B_r] = \begin{bmatrix} [0] \\ [M]^{-1} \end{bmatrix}_{2 \times 1} \quad (28)$$

Using the closed-loop feedback control layout, Equation 24 can be mathematically solved. Then, the control force vector is obtained by feeding back the structural response measurements. Therefore, the feedback law can be described as follows:

$$[u(t)]_{1 \times 1} = -[G]_{1 \times 2}[Z(t)]_{2 \times 1} \quad (29)$$

Where $[G]$ is feedback gain matrix with a dimension of $r \times 2n$. Using these r extra equations, the control system response, i.e. $[Z(t)]$, can be obtainable from Equation 24. Substituting Equation **Error! Reference source not found.**29 into Equation **Error! Reference source not found.**24, leads to the following equation:

$$[\dot{Z}(t)] = [A_c][Z(t)] + [B_r][\ddot{x}_g(t)] \quad (30)$$

Where,

$$[A_c] = [A] - [B_u][G] \quad (31)$$

In the abovementioned equations, $[A]$ is plant matrix of uncontrolled system, $[A_c]$ is the closed-loop plant matrix of the system. As denoted above, if all the state variables of the system are measured, the closed-loop system would become a full-state feedback [6]. In smart structures, measuring the state variables, i.e. displacements and velocities, is difficult. As a suitable replacement, measuring the accelerations can be very reliable in seismic response control systems. There is some research in this issue indicating the achievement of direct acceleration feedback [37-41]. Using this method causes simplicity in the sensing system, which leads the achievement of more practical control systems. It has been expressed that the closed-loop feedback control layout is the most popular and suitable feedback control layout in smart structures. In this numerical analysis, the closed-loop feedback control layout has been selected to be installed in both systems, i.e. the toggle and tendon control systems [6]. The schematic layout for closed-loop control has been shown in Figure 11.

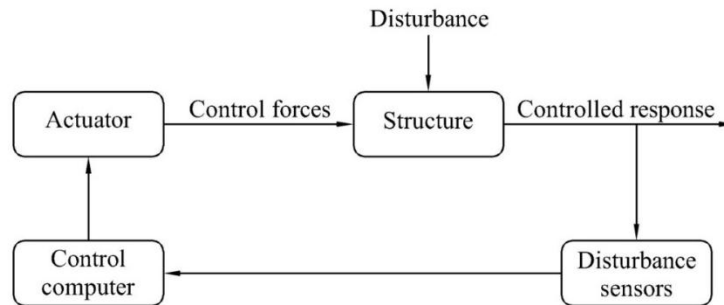


Fig.11. Schematic layout for closed-loop control.

9.1.7. Control algorithm in smart structures

In active control systems, the active control force is determined using active control algorithms based on the sensed structural response. The control algorithms are installed in electronic devices called either digital controller or control computer. For the active control systems, the mathematical model of the controller is known as control law. Also, installation of the control algorithm in an active control system is named controller design. In this investigation, known algorithms of *LQR* and pole placement have been used through the especial functions in MATLAB® [6].

9.1.8. Earthquake acceleration data

The earthquake data which has been applied to both active control systems are 1979 Imperial Valley–El Centro M (6.5) and 1994 Northridge M (6.7). These earthquake accelerations are presented in Fig. 12 and Fig. 13, respectively. Since the strongest motions typically occur early in historical earthquakes, only the first 20 seconds of their accelerations are shown in these figures. These earthquake data can be obtained from the website of the Pacific Earthquake Engineering Research Centre.

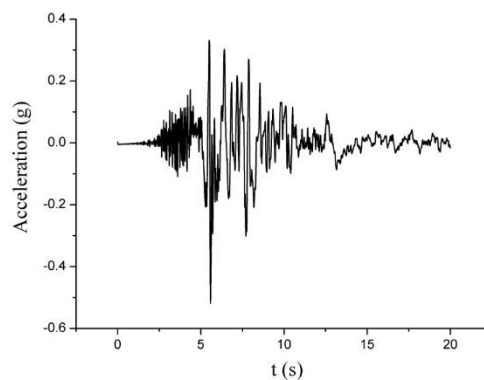


Fig. 12. 1979 El Centro earthquake accelerations.

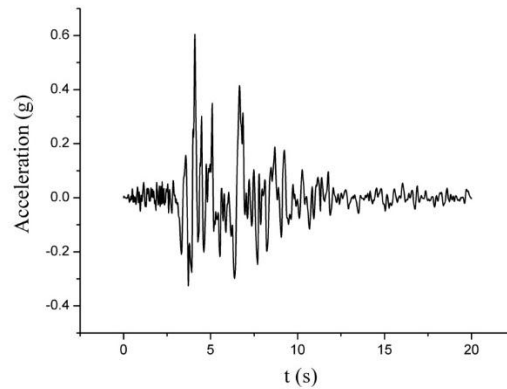


Fig. 13. 1994 Northridge earthquake accelerations.

9.1.9. Control gain matrix in active Toggle control system

For the active toggle control system, the state form of motion equation is obtained as follows. The following relationships have already been discussed in previous sections. Notice that in these equations, $\alpha = 9.6$ is the toggle coefficient which has been already calculated.

$$[\dot{Z}(t)] = [A_c][Z(t)] + [B_r][\dot{x}_g(t)], [B_r] = \begin{bmatrix} 0 \\ [M]^{-1}[\delta] \end{bmatrix}_{2n \times 1} \quad (32)$$

$$[A_c] = [A] - [\alpha B_u][G] \quad (33)$$

$$[A] = \begin{bmatrix} 0 & 1 \\ -\frac{589}{12} & -\frac{3.4}{12} \end{bmatrix} \quad (34)$$

$$[B_u] = \begin{bmatrix} 0 \\ -\alpha \frac{1}{12} \end{bmatrix} \quad (35)$$

For finding the control gain matrix $[G]$ in the closed-loop control system, the function of *LQR* in MATLAB[®] software is used as follows:

$$[G] = \text{LQR}(A, B_u, Q, R) \quad (36)$$

In the above mentioned equation, all the terms inside the parentheses are matrices and have the same characteristics as those explained previously. However, matrices $[Q]$ and $[R]$ are known as weighting matrices and in this calculation process are tuned to be as follows:

$$[Q] = \begin{bmatrix} 10 & 0 \\ 0 & 10 \end{bmatrix} \quad (37)$$

$$[R] = [0.001] \quad (38)$$

Using the *PLACE* function in MATLAB[®], for providing the more stability of the system, poles of the system are designed to be -150 , identically. Therefore, the gain matrix for the closed-loop control system is as follows:

$$[G_{Toggle}] = [-28114 \quad -375] \quad (39)$$

9.1.10. Control gain matrix in active tendon control system

Determining the gain matrix in the active tendon control system would be the same as the procedure expressed for the active toggle control system. Notice that in the tendon system, all parameters are identical to the toggle model. Using the same poles considered in the active toggle control system, i.e. -150 , the gain matrix in active tendon control system will be as follows:

$$[G_{Tendon}] = \alpha[G_{Toggle}] = 9.6[G_{Toggle}] \quad (40)$$

9.1.11. Determination of structural displacement response

The state vector $[Z(t)]$, can be solved easily using *LSIM* function in MATLAB® software package. In this procedure, it is assumed that the control force $[u(t)]$ is known. In an optimal closed-loop control system, optimal control force $[u(t)]$ is adjusted based only on the feedback of $[Z(t)]$, i.e. the state vector comprising the displacements and velocities. Therefore, to attain the state vector, the relevant response in the building structure must be measured at time instant t by installing the displacement and velocity sensors at the proper locations on each floor. Since the specifications of the two systems, i.e. toggle and tendon systems, have been considered identical, the derived structural displacement responses for both systems would be the same. These structural responses due to the applied earthquake excitations can be calculated using the function *LSIM* in MATLAB® software as follows:

$$[Y, Z] = LSIM(A_c, B_r, S, \ddot{x}_g, T) \quad (41)$$

In the aforementioned equation, A_c is called the closed-loop plant matrix of the system, B_r and \ddot{x}_g have been already explained in the relevant sections. However, matrices $S = [1 \quad 1]$ and T are the sensor matrix and the simulation time matrix, respectively. The structural displacement responses, i.e. the displacements of top of the frames for 1979 El Centro and 1994 Northridge earthquakes, are shown in Fig.14 and Fig.15, respectively. The absolute maximum controlled structural displacement under 1979 El Centro and 1994 Northridge earthquakes are 0.22 mm and 0.25 mm , respectively.

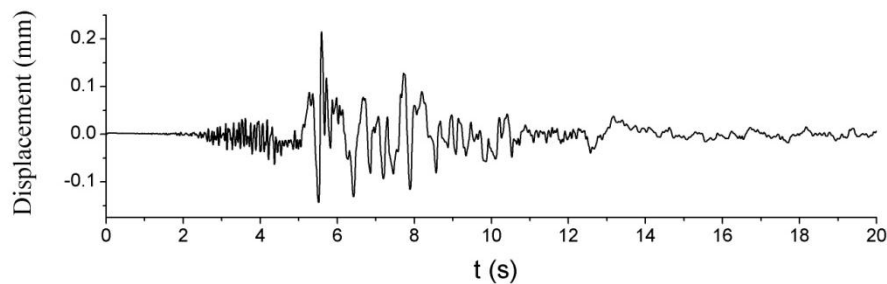


Fig.14. Controlled structural displacement response under 1979 El Centro earthquake.

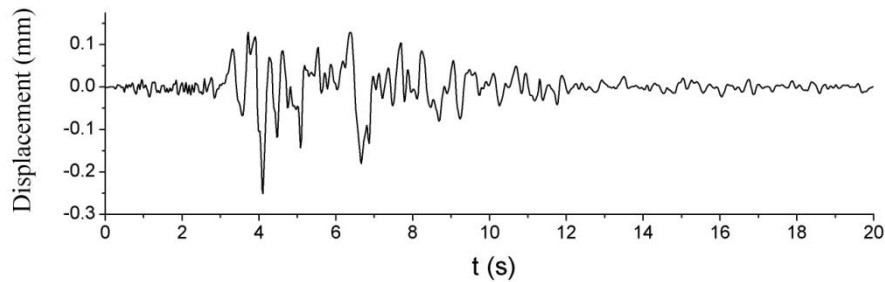


Fig.15. Controlled structural displacement response under 1994 Northridge earthquake.

9.1.12. Calculation of control forces

After obtaining the control gain matrix, the required control forces for both systems can be determined using Equation **Error! Reference source not found.**29. Notice that in this equation, the control gain matrix has been obtained by using *LQR* algorithm. Therefore, the equation for determining the control forces in both systems is written as follows:

$$[u(t)] = -[G][Z(t)] \quad (42)$$

In the above mentioned equation, the matrices $[G]$ and $[Z(t)]$ have already been determined for the relevant systems individually, as explained in the previous sections.

10. Comparing results for numerical process

10.1. Actuator forces

In this section, after determining the control forces or, in the other words, the actuator forces in the active toggle and tendon control systems, these control forces have been plotted on graphs and shown in Fig.16 and Fig.17 to demonstrate the difference between the relevant results.

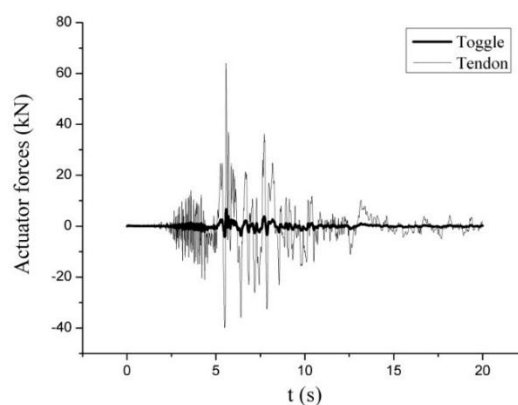


Fig.16. Compared control forces in 1979 El Centro Earthquake.

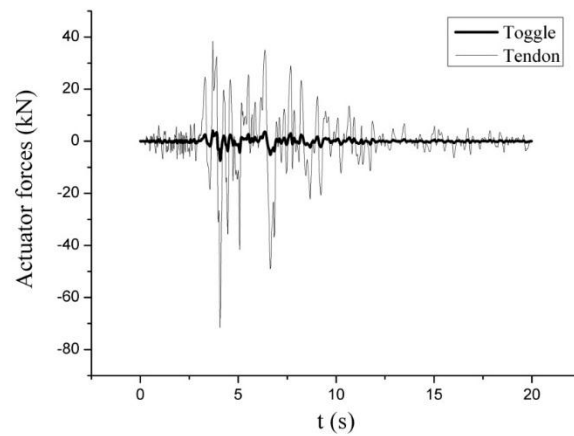


Fig.17. Compared control forces in 1994 Northridge Earthquake.

It is obvious from Fig.16 and Fig.17 that an active control system with the toggle configuration can enormously diminish the required actuator forces. In this numerical analysis, this reduction is about 89.6%, compared to the tendon control system with various seismic excitations. Also, having the toggle coefficient, this reduction in the control forces in the toggle system can be achieved directly from Equation12.

10.2. Displacements

The compared results related to the controlled and uncontrolled displacements have been plotted in Fig.18 and Fig.19 for 1979 El Centro and 1994 Northridge earthquakes, respectively. The responses for the free vibration have been calculated by the methods based on interpolation of excitation [36].

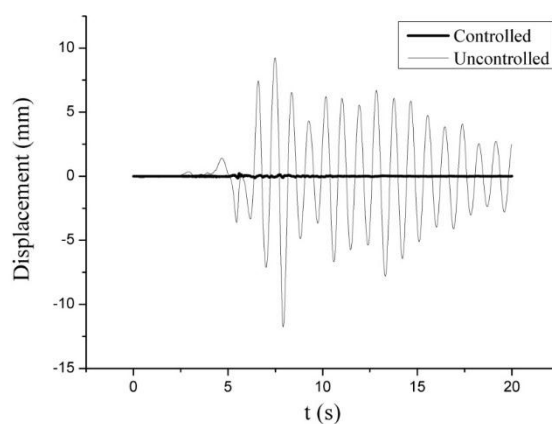


Fig.18. Compared frame displacements in 1979 El Centro earthquake.

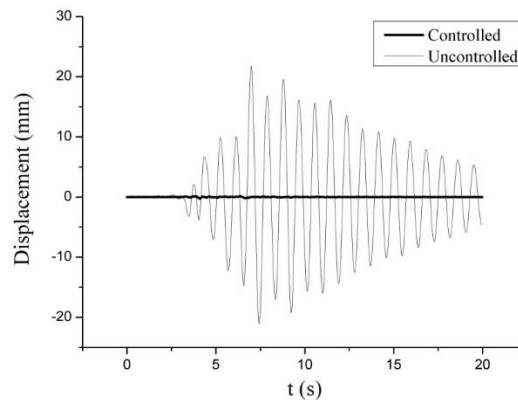


Fig.19. Compared frame displacements in 1994 Northridge earthquake.

It is obvious from Figures 18 and 19 that deploying the toggle configuration in an active control system can enormously diminish the structural responses under the earthquake vibrations.

11. Conclusions

- 1-The installation of the toggle configuration in a single-degree-of-freedom shear frame in an active control system causes a coefficient called toggle coefficient α to be created. This coefficient appears in the motion equation of the system as a direct factor multiplied to the control force.
- 2-For the typical civil engineering frames, the value of toggle coefficient α is greater than unity.
- 3-In this system, the greater toggle coefficient α generates the smaller control force.
- 4-In the toggle configuration, θ_1 and L_1 are independent values. It means that all other geometrical characteristics can be calculated from the geometry of the system after selecting values for θ_1 and L_1 .
- 5-The proper establishment of the motion equation in the toggle system depends on suitable values for θ_1 to θ_3 and L_1 . Otherwise, the toggle configuration of the active control system will no longer be valid. Moreover, the system works as a toggle configuration in the active control system if $\theta_1 + \theta_2 < 90^\circ$.
- 6-To have the more efficient active toggle control system, the smaller value for the lower brace, i.e. L_1 becomes desirable. This is because the smaller L_1 generates the greater α .
- 7-In the design procedure in the active toggle control system, it is beneficial to select the frames with bigger spans, since the greater span produces the bigger toggle coefficient α .
- 8-In the design procedure in the active toggle control system, it is preferable to keep the frame height as low as possible, since the greater height generates the smaller toggle coefficient α .
- 9-The toggle system acts more efficiently in θ_1 s that are close to their maximum values. This property can be used to reach the much greater toggle coefficient. However, the toggle establishment criterion, i.e. $\theta_1 + \theta_2 < 90^\circ$ and construction restrictions have to be taken into consideration.
- 10-Comparison between control forces in the toggle and tendon control systems shows an 89.6% reduction for the former. As a result, the toggle configuration significantly reduces the force required from the actuator; consequently the size of the actuator and its cost will be reduced.

12. References

- 1.Xu, Y. L., Teng, J., (2002). Optimum design of active/passive control devices for tall buildings under earthquake excitation. *The Structural Design of Tall Buildings*, 11(2),109-127.
- 2.Yang, J., Soong, T., (1988). Recent advances in active control of civil engineering structures. *Probabilistic engineering mechanics*, 3(4), p. 179-188.
- 3.Soong, T., (1988). State-of-the-art review: Active structural control in civil engineering. *Engineering Structures*, 10(2), p. 74-84.
4. Housner, G. W., Bergman, L. A., Caughey, T. K., Chassiakos, A. G., Claus, R. O., Masri, S. F., Skelton, R. E., Soong, T. T., Spencer, B. F. J., Yao, T. P., (1997). Structural control: past, present, and future. *Journal of Engineering Mechanics*, 123(9), 897-971.
5. Spencer Jr. B., Nagarajaiah, S., (2003). State of the art of structural control. *Journal of Structural Engineering*, 129(7), 845-856.
6. Cheng, F. Y., Jiang, H., Lou, K., (2010). *Smart structures: Innovative systems for seismic response control*. CRC Press.

7. Wu, B., Ou, J. P., Soong, T. T., (1997). Optimal placement of energy dissipation devices for three-dimensional structures. *Engineering Structures*, 19(2), 113-125.
8. Spencer Jr. B., Sain, M. K., (1997). Controlling buildings: a new frontier in feedback. *Control Systems, IEEE*, 17(6), 19-35.
9. Yamazaki, S., Nagata, N., Abiru, H., (1992). Tuned active dampers installed in the Minato Mirai (MM) 21 landmark tower in Yokohama. *Journal of Wind Engineering and Industrial Aerodynamics*, 43(1), 1937-1948.
10. Cao, H., Reinhorn, A. M., Soong, T. T., (1998). Design of an active mass damper for a tall TV tower in Nanjing, China. *Engineering Structures*, 20(3), 134-143.
11. Kareem, A., Kijewski, T., Tamura, Y., (1999). Mitigation of motions of tall buildings with specific examples of recent applications. *Wind and Structures*, 2(3), 201-251.
12. Ikeda, Y., Sasaki, K., Sakamoto, M., Kobori, T., (2001). Active mass driver system as the first application of active structural control. *Earthquake engineering & structural dynamics*, 30(11), 1575-1595.
13. Yamamoto, M., Aizawa, S., Higashino, M., Toyama, K., (2001). Practical applications of active mass dampers with hydraulic actuator. *Earthquake Engineering & Structural Dynamics*, 30(11), 1697-1717.
14. Ricciardelli, F., Pizzimenti, A. D., Mattei, M., (2003). Passive and active mass damper control of the response of tall buildings to wind gustiness. *Engineering Structures*, 25(9), 1199-1209.
15. Park, W., Soon Park, K., Moo Koh, H., Ho Ha, D., (2006). Wind-induced response control and serviceability improvement of an air traffic control tower. *Engineering Structures*, 28(7), 1060-1070.
16. Abe, M., Fujino, Y., (1994). Dynamic characterization of multiple tuned mass dampers and some design formulas. *Earthquake engineering & structural dynamics*, 23(8), 813-835.
17. Amini, F., and Tavassoli, M. R., (2005). Optimal structural active control force, number and placement of controllers. *Engineering Structures*, 27(9), 1306-1316.
18. Liu, D. K., Yang, Y. L., Li, Q. S., (2003). Optimum positioning of actuators in tall buildings using genetic algorithm. *Computers & Structures*, 81(32), 2823-2827.
19. Park, W., Park, K. S., Koh, H. M., (2008). Active control of large structures using a bilinear pole-shifting transform with control method. *Engineering Structures*, 30(11), 3336-3344.
20. Pantelides, C. P., Cheng, F. Y., (1990). Optimal placement of controllers for seismic structures. *Engineering Structures*, 12(4), 254-262.
21. Cheng, F. Y., (1988). Response Control Based on Structural Optimization and its Combination with Active Protection. In *Proceeding of 9th World conference in Earthquake engineering*, IAEE, Tokyo, 3, 471.
22. Rama Mohan Rao, A., Sivasubramanian, K., (2008). Optimal placement of actuators for active vibration control of seismic excited tall buildings using a multiple start guided neighbourhood search (MSGNS) algorithm. *Journal of Sound and Vibration*, 311(1-2), 133-159.
23. Soong, T. T., Dargush, G. F., (1997). *Passive energy dissipation systems in structural engineering*. Wiley.
24. Council, B. S. S., (2000). *Prestandard and commentary for the seismic rehabilitation of buildings*, FEMA-356. Federal Emergency Management Agency, Washington, DC.
25. Constantinou, M. C., Symans, M., (1992). Experimental and analytical investigation of seismic response of structures with supplemental fluid viscous dampers. *National Center for earthquake engineering research*.
26. Hwang, S. J., Huang, Y. N. Y., Hung, H., J. C., (2004). Applicability of seismic protective systems to structures with vibration-sensitive equipment. *Journal of Structural Engineering*, 130(11), 1676-1684.
27. Reinhorn, A. M., Viti, S., Cimellaro, G., (2005). Retrofit of structures: Strength reduction with damping enhancement. in *Proceedings of the 37th UJNR panel meeting on wind and seismic effects*.
28. Soong, T., Spencer, B., (2002). Supplemental energy dissipation: state-of-the-art and state-of-the-practice. *Engineering Structures*, 24(3), 243-259.
29. Constantinou, M. C., Tsopelas, P., Hammel, W., Sigaher Ani, N., (2001). Toggle-brace-damper seismic energy dissipation systems. *Journal of Structural Engineering*, 127(2), 105-112.
30. Sigaher, A. N., Constantinou, M. C., (2003). Scissor-jack-damper energy dissipation system. *Earthquake Spectra*, 19(1), 133-158.
31. Hwang, J. S., Huang, Y. N., Hung, Y. H., (2005). Analytical and experimental study of toggle-brace-damper systems. *Journal of structural engineering*, 131(7), 1035-1043.
32. Chung, L., Reinhorn, A., Soong, T., (1988). Experiments on active control of seismic structures. *Journal of Engineering Mechanics*, 114(2), 241-256.
33. Chung, L. L., Lin, R. C., Soong, T. T., Reinhorn, A. M., (1989). Experimental study of active control for MDOF seismic structures. *Journal of Engineering Mechanics*, 115(8), 1609-1627.
34. Cheng, F. Y., Jiang, H., (1998). Optimum control of a hybrid system for seismic excitations with state observer technique. *Smart materials and structures*, 7(5), 654.
35. Cheng, F. Y., Jiang, H., (1998). Hybrid control of seismic structures with optimal placement of control devices. *Journal of Aerospace Engineering*, 11(2), 52-58.
36. Chopra, A. K., (2001). *Dynamics of structures: Theory and applications to earthquake engineering*. 2, Prentice Hall Saddle River, eNY NY.
37. Dyke, S. J., Quast, P., Sain, M. K., Soong, T. T., (1994). Absolute acceleration feedback control strategies for the active mass driver. in *Proc. First World Conference on Structural Control*.
38. Dyke, S. J., Spencer, B. F. Jr., Quast, P., Sain, M. K., Kaspari, D. C. Jr., Soong, T. T., (1994). Experimental verification of acceleration feedback control strategies for an active tendon system. *National Center for Earthquake Engineering Research*.
39. Dyke, S. J., Quast, P., Sain, M. K., Soong, T. T., (1996). Acceleration feedback control of MDOF structures. *Journal of engineering mechanics*, 122(9), 907-918.
40. Dyke, S. J., Quast, P., Sain, M. K., Soong, T. T., (1996). Implementation of an active mass driver using acceleration feedback control. *Computer-Aided Civil and Infrastructure Engineering*, 11(5), 305-323.
41. Spencer Jr. B. F., Quast, P., Dyke, S. J., Sain, M. K., (1994). *Digital Signal Processing Techniques for Active Structural Control*. *Proceeding of the 1994 ASCE Structures Congress*, Atlanta, Georgia.